

Searching for neutral particles at the highest energies at the Pierre Auger Observatory

Marcus Niechciol^{1,*} for the Pierre Auger Collaboration^{2,**,***}

¹Center for Particle Physics Siegen, University of Siegen, Walter-Flex-Str. 3, 57072 Siegen, Germany

²Observatorio Pierre Auger, Av. San Martín Norte 304, 5613 Malargüe, Argentina

Abstract. The Pierre Auger Observatory, being the largest air-shower experiment in the world, offers an unprecedented exposure to neutral particles at the highest energies. Since the beginning of data collection more than 18 years ago, several searches for ultra-high-energy (UHE, $E > 10^{17}$ eV) photons and neutrinos have been performed. The upper limits on the diffuse flux of UHE photons and neutrinos derived from Auger data are among the most stringent in the world, severely constraining models for the origin of UHE cosmic rays. In addition, the Pierre Auger Observatory contributes to current efforts in multimessenger astronomy through follow-up searches for UHE photons and neutrinos in association with transient events, such as gravitational wave events. The various activities concerning searches for UHE photons and neutrinos in the data from the Pierre Auger Observatory are presented and the current results are summarized. In addition, future perspectives will be discussed.

1 Introduction

Neutral particles, in particular photons and neutrinos, play a crucial role for current efforts in multimessenger astronomy, where one of the main goals is understanding where and how ultra-high-energy (UHE, commonly referring to the energy range above $\sim 10^{17}$ eV) cosmic rays are produced. These particles can even exceed energies of 10^{20} eV, far beyond what can be reached with man-made particle accelerators. One can exploit the intimate connection between UHE cosmic rays and UHE photons and neutrinos, which appear as “by-products” in almost every scenario aiming at explaining UHE cosmic rays, originating either directly at the sources (“astrophysical” photons and neutrinos) or during the propagation of the UHE cosmic rays through the Universe (“cosmogenic” photons and neutrinos). Photons and neutrinos themselves are complementary messengers: Photons trace the local Universe up to Mpc scales, due to interactions with the cosmic background fields, while neutrinos can traverse the whole Universe. In addition, neutral particles at the highest energies can also serve as cosmic probes of fundamental physics and open a window to new physics, for example in the context of super-heavy dark matter, violations of Lorentz invariance, or axions.

Just as for UHE cosmic rays, also the fluxes of UHE neutral particles are far too small for direct detection using, e.g., satellite experiments. However, photons and neutrinos entering the Earth’s atmosphere can initiate exten-

sive air showers like a charged cosmic ray, making indirect detection possible. Therefore, a cosmic-ray observatory measuring air showers can, by construction, also be a photon observatory and even a neutrino observatory, complementing specialized instruments and adding valuable pieces of information to current multimessenger studies.

In these proceedings, current searches for UHE photons and neutrinos with data collected by the Pierre Auger Observatory are summarized. The Observatory itself is briefly introduced in Sec. 2. Sec. 3 deals with searches for UHE photons, while Sec. 4 focusses on UHE neutrinos, including an update of the limits on the diffuse flux of neutrinos with data until the end of 2021. A brief summary is given in Sec. 5, including a discussion of future prospects with the on-going detector upgrade of the Observatory, dubbed AugerPrime.

2 The Pierre Auger Observatory

The Pierre Auger Observatory [1], located near the town of Malargüe in the Argentinian *Pampa Amarilla*, is the largest cosmic-ray observatory to date. A key feature of the Pierre Auger Observatory is the hybrid concept, combining a Surface Detector array (SD) with a Fluorescence Detector (FD). The SD consists of about ~ 1600 water-Cherenkov detectors arranged on a triangular grid with a spacing of 1500 m, covering a total area of about 3000 km^2 . The SD is overlooked by 24 fluorescence telescopes, located at four sites at the border of the array. The SD samples the lateral shower profile at ground level, i.e., the distribution of particles as a function of the distance from the shower axis, with a duty cycle of $\sim 100\%$, while the FD records the longitudinal shower development in

*e-mail: niechciol@physik.uni-siegen.de

**e-mail: spokespersons@auger.org

***Full author list: https://www.auger.org/archive/authors_2022_10.html

the atmosphere above the SD. The FD can only be operated in clear, moonless nights, reducing the duty cycle to $\sim 15\%$. In the western part of the SD array, ~ 50 additional SD stations have been placed between the existing SD stations, forming a sub-array with a spacing of 750 m and covering a total area of about 27.5 km^2 . With this sub-array, air showers of lower primary energy (below 10^{18} eV) with a smaller footprint on the ground can be measured. To allow also for hybrid measurements in this energy range, where air showers develop above the field of view of the standard FD telescopes, three additional High-Elevation Auger Telescopes (HEAT) have been installed at the FD site Coihueco, overlooking the 750 m SD array. The HEAT telescopes operate in the range of elevation angles from 30° to 60° , complementing the Coihueco telescopes operating in the 0° to 30° range. The combination of the data from both HEAT and Coihueco (“HeCo” data) enables fluorescence measurements of air showers over a large range of elevation angles.

3 Searches for UHE photons

The biggest challenge when searching for UHE neutral particles is to distinguish air showers initiated by these primaries from those induced by the vast background of primary protons and heavier nuclei in cosmic rays. For the identification of primary photons, one can exploit the fact that the development of photon-induced air showers in the atmosphere is dominated by electromagnetic interactions, which leads to two key differences with respect to air showers initiated by protons and nuclei (for a review, see [2]). Firstly, the atmospheric depth of the shower maximum X_{max} lies deeper in the atmosphere, due to the lower multiplicity of electromagnetic interactions compared to hadronic interactions. Secondly, fewer secondary muons are produced, as only a small fraction of the total energy is transferred to the hadronic (and subsequent muonic) channel through photo-nuclear interactions. One consequence of this is a steeper lateral distribution of secondary particles on the ground and a smaller overall footprint of the shower.

At the Pierre Auger Observatory, these key differences are exploited in various searches for photons. We will focus here on searches for a diffuse—i.e., direction-independent, unresolved—flux of photons, which are performed in three different energy ranges: between 2×10^{17} and 10^{18} eV, using HeCo data combined with data from the 750 m SD array [3]; between 10^{18} and 10^{19} eV using data from the main fluorescence telescopes and the 1500 m SD array [4]; and above 10^{19} eV using only data from the 1500 m SD array [5]. In addition, two searches for point sources of UHE photons have been performed: a blind search covering the full field of view of the Observatory [6] and a targeted search involving different classes of potential sources [7]. Both of these analyses are not discussed here further and are only mentioned for completeness. Also dedicated multimessenger studies involving UHE photons have been published, such as follow-up searches for photons in coincidence with transient events like gravitational wave events [8] or the anomalous blazar

TXS 0506+056 [9]. These multimessenger analyses are the subject of another contribution [10]. A more detailed summary of all searches for UHE photons at the Pierre Auger Observatory can be found in [11].

In the following, the three searches for a diffuse flux of photons mentioned before are briefly described. In the energy range between 2×10^{17} and 10^{18} eV, the analysis is based on three observables: X_{max} , S_b and N_{stations} . X_{max} can be measured directly with the fluorescence telescopes, while S_b is calculated from the SD measurement through

$$S_b = \sum_i S_i \times \left(\frac{R_i}{1000 \text{ m}} \right)^b,$$

where S_i and R_i denote the measured signal and the perpendicular distance to the shower axis of the i -th triggered station in a given SD event and the parameter b was fixed to 4 [12]. N_{stations} is the number of triggered stations in the event. Both S_b and N_{stations} can be seen as a measure of the steepness of the lateral distribution and hence add complementary information to X_{max} , which depends on the longitudinal development of the air shower. These three observables are combined in a multivariate analysis. The output of the boosted decision tree (BDT) analysis, β , is plotted in Fig. 1(a). The BDT is trained using large samples of photon- and proton-induced air showers. The final value of the photon candidate cut was chosen to ensure a signal efficiency of 50%. At this signal efficiency, the background rejection (determined from proton simulations) is about 99.9%. Eventually, the analysis was applied to data collected between 1 June 2010 and 31 December 2015. No events from the data sample pass the candidate cut, hence, upper limits on the incoming photon flux are determined, based on an exposure to photons of about $2.5 \text{ km}^2 \text{ sr yr}$ in the given energy range and for the given time period.

The search for photons between 10^{18} and 10^{19} eV is also based on X_{max} , but complemented by the observable F_μ , which is a proxy for the muon content of the air shower [13]. F_μ is calculated using a model based on air-shower universality, taking the measured signals in the SD stations as input as well as the shower geometry and X_{max} reconstructed from the FD. The combination of both observables in a Fisher discriminant analysis (see Fig. 1(b)) yields an overall background rejection (at a signal efficiency of 50%) of about 99.9%. The analysis is then applied to data from the period 1 January 2005 to 31 December 2017, which is equivalent to an exposure to UHE photons of about $1000 \text{ km}^2 \text{ sr yr}$. A total of 22 events from the data sample passed the candidate cut. However, this number is fully compatible with the expectation, determined *a priori* from a sub-sample of the data set which was not used in the final analysis, of 30 ± 15 events. These candidate events were studied in detail, yet none of them could be identified unambiguously as being initiated by a primary photon.

In the energy range above 10^{19} eV, the statistics of the data sample collected by the FD is not sufficient anymore to efficiently search for UHE photons. The SD, with a duty cycle of nearly 100%, can provide much better statistics at the highest energies. The lack of a corresponding FD

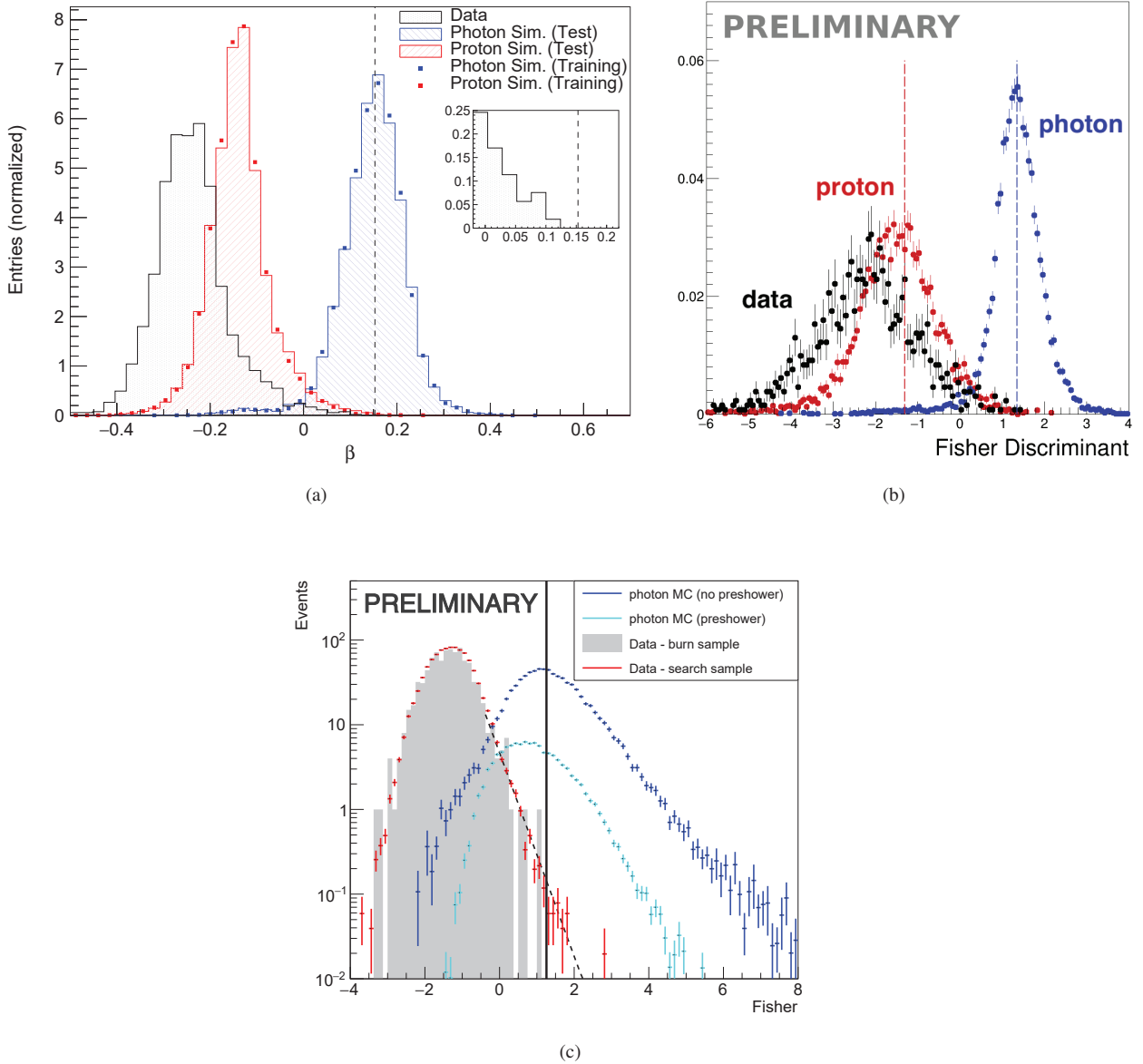


Figure 1. Results of the multivariate analyses used to search for primary photons in the data collected by the Pierre Auger Observatory; (a) energy range between 2×10^{17} and 10^{18} eV, using HeCo data combined with data from the 750 m SD array [3]; (b) energy range between 10^{18} and 10^{19} eV using data from the main fluorescence telescopes and the 1500 m SD array [4]; (c) energy range above 10^{19} eV using only data from the 1500 m SD array [5].

for the bulk of the data, however, poses some challenges. For example, there is no measurement of X_{\max} available. Also, the energy of the primary particle can only be determined indirectly. Here, we use a look-up table constructed with a large sample of photon-induced air showers. Two observables, L_{LDF} and Δ , are used in this analysis. L_{LDF} quantifies the departure of the observed lateral distribution function (LDF) from the average of all SD data:

$$L_{\text{LDF}} = \log_{10} \left(\frac{1}{N} \sum_{i=1}^N \frac{S_i}{f_{\text{LDF}}(r_i)} \right),$$

where S_i is the total signal measured in the i -th SD station and $f_{\text{LDF}}(r_i)$ gives the average signal, obtained from all SD data, for a station at the same distance r_i from the shower

axis. Δ is defined through:

$$\Delta = \frac{1}{N} \sum_i \frac{(t_{1/2}^i - t_{1/2}^{\text{bench}})}{\sigma_{t_{1/2}}},$$

which can be taken as the average deviation of the measured rise-times from a *data benchmark* $t_{1/2}^{\text{bench}}$, describing the average risetime of all of the SD data (assumed to be overwhelmingly constituted by primary nuclei), in units of sampling fluctuations $\sigma_{t_{1/2}}$. The use of the average behavior of all SD data in the two quantities removes the need for assumptions on the composition of the background, which is not known in detail at the highest energies. The two observables are combined in a Fisher discriminant analysis, with the burnt sample—about 2 %

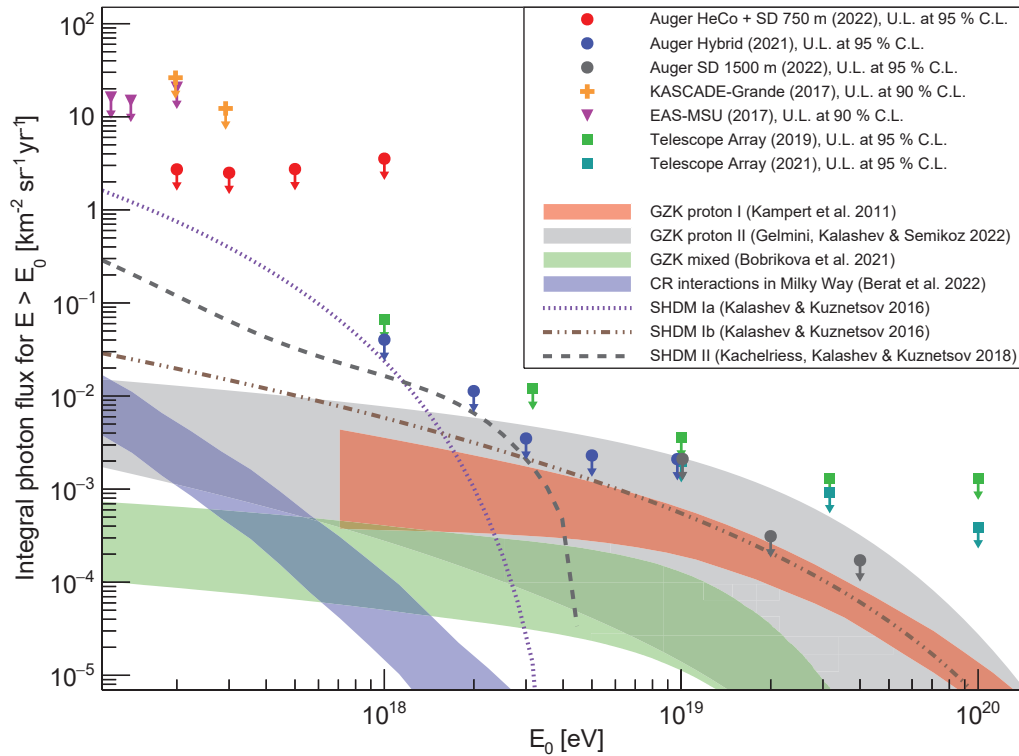


Figure 2. Current upper limits on the integral photon flux determined from data collected by the Pierre Auger Observatory (red, blue and gray circles); shown are also upper limits published by other experiments as well as the expected photon fluxes under different theoretical assumptions and scenarios; for a full list of references, see [11].

of the full data sample which are not used in the final analysis—representing the background and photon simulations the signal (see also Fig. 1(c)). The analysis is finally applied to SD data collected between 1 January 2004 and 30 June 2020, which corresponds to an exposure of about $17000 \text{ km}^2 \text{ sr yr}$. Overall, 16 events from the data sample pass the photon candidate cut, which is consistent with the expectation. Again, no primary photon could be unambiguously identified.

The upper limits on the integral photon flux determined through the three analyses discussed before are shown in Fig. 2, together with upper limits determined from other experiments as well as the expected photon fluxes under different theoretical assumptions and scenarios. The upper limits determined by the Pierre Auger Observatory are the most stringent ones to date, over a wide energy range spanning from $2 \times 10^{17} \text{ eV}$ to the highest energies. More “exotic”, top-down models have been strongly constrained—a number of such models were, in fact, already ruled out by previous results published by the Pierre Auger Collaboration. On the other hand, the predictions from some cosmogenic models, for example involving interactions of UHE cosmic rays with the cosmic microwave background, are within reach. For a more detailed discussion of the astrophysical significance of these limits, see [11]. However, we note here that upper limits on the diffuse flux of photons are especially useful to constrain theoretical models involving super-heavy dark matter (see, e.g., [14, 15]).

4 Searches for UHE neutrinos

In a nutshell, searching for UHE neutrinos in air-shower data means searching for inclined showers with an electromagnetic component. Protons and nuclei initiate air showers high in the atmosphere. At large zenith angles, the electromagnetic component is fully absorbed within the atmosphere, and only muons arrive on the ground. Neutrinos, on the other hand, have a much smaller interaction cross section and can thus also initiate showers much deeper in the atmosphere, close to the ground, so that the electromagnetic component of the shower can still be measured even at large zenith angles. This leads to a unique signature that can be efficiently detected with a ground array. Another search channel comes from Earth-skimming τ neutrinos interacting in the Earth’s crust, producing a τ lepton that enters the atmosphere from below and initiates a slightly upgoing air shower close to the ground—again, a unique signature.

All searches for UHE neutrinos at the Pierre Auger Observatory are based on these signatures. The analyses are categorized into three search channels, based on the zenith angle: Earth-skimming (ES, zenith angles between 90° and 95°); down-going high angle (DGH, zenith angles between 75° and 90°) and down-going low-angle (DGL, zenith angles between 60° and 75°). The down-going channels are further subdivided into a number of sub-channels based on the number of triggered SD stations in the event (for the DGH channel) or based on the zenith angle (for the DGL channel). Using the combined results

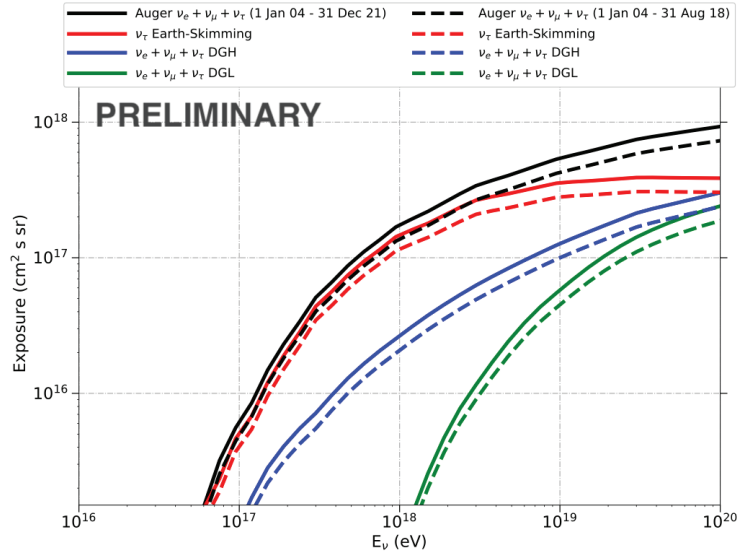


Figure 3. Exposure of the 1500 m SD array to UHE neutrinos as a function of energy, for the three search channels (ES, DGH, DGL) and the data period 1 January 2004 to 31 December 2021 (solid lines); for comparison, also the corresponding exposure for the data period from [16] is included (dashed lines).

of all three search channels, upper limits on the diffuse flux of UHE neutrinos have been obtained using data from the 1500 m SD array collected between 1 January 2004 and 31 August 2018 [16]. Here, we update these results with data until 31 December 2021. In addition, limits on point-like sources of UHE neutrinos have been determined [17], which are not discussed further here. Follow-up searches for UHE neutrinos from transient events constitute an important contribution of the Pierre Auger Observatory to current multimessenger studies, in particular for gravitational wave events (see, e.g., [18]). We note again that these multimessenger analyses are summarized in [10].

As mentioned before, we update here our results from [16] with about 3.5 more years of data, which constitutes approximately a 30 % increase in exposure. The exposure to neutrinos, as a function of energy and determined from simulations, is shown in Fig. 3, divided into the three search channels and compared to the exposure from [16]. The exposure is dominated by the ES channel up to about 4×10^{19} eV, then the down-going channels take over.

As examples, we show the results of the data unblinding in two search channels in Fig. 4. In the ES channel (Fig. 4(a)), the average area-over-peak $\langle \text{AoP} \rangle$, defined as the ratio of the integral of the time trace in a SD station to its peak value, averaged over all triggered stations in an SD event, is used as the discriminating observable. The neutrino candidate cut is chosen based on a subset of the data sample, such that a false-positive rate of one event per 50 years is expected. At this cut value, the neutrino selection efficiency is about 95 %. In Fig. 4(b), the results of the unblinding in the DGH channel, specifically the sub-channel with $N_{\text{stations}} \in [7, 11]$, is shown. In the DGL and DGH channels, the analysis is again based on the AoP values, but in this case, several observables that carry

information on the time spread of the signals in the SD stations are constructed from the individual AoP values and subsequently combined in a Fisher discriminant analysis. The neutrino candidate cut is independently optimized for each sub-channel, again ensuring a false-positive rate of one event in 50 years. In the specific sub-channel shown in Fig. 4(b), the neutrino selection efficiency is about 85 %. No neutrino candidate event has been identified in any of the search channels.

From the non-observation of any neutrino event, upper limits on the diffuse flux of neutrinos are determined. Assuming a (single flavor) neutrino flux of the form $\phi = k \times E_{\nu}^{-2}$, an upper limit on the normalization k , for the energy range between 10^{17} and 2.5×10^{19} eV, was obtained at $3.5 \times 10^{-9} \text{ GeV cm}^{-2} \text{ s}^{-1} \text{ sr}^{-1}$ or, equivalently, $1.1 \text{ EeV km}^{-2} \text{ yr}^{-1} \text{ sr}^{-1}$. Since no neutrino candidate events have been identified, the increased exposure from the larger data set directly translate into an improvement of the upper limit on k . Upper limits can also be determined for energy bins of width 0.5 in $\log_{10}(E_{\nu} / \text{eV})$. These (differential) limits are an effective way of characterizing the energy dependence of the sensitivity of a neutrino experiment. For the Pierre Auger Observatory, the best sensitivity is achieved at energies around 10^{18} eV, where it becomes comparable to that of IceCube. Both the integral and differential upper limits are shown in Fig. 5, together with upper limits determined by the IceCube and ANITA experiments, as well as the expected neutrino fluxes under different theoretical assumptions and scenarios. Using these results, we can constrain several classes of models of neutrino production, both cosmogenic and astrophysical. In particular, cosmogenic models involving a pure-proton composition and a strong evolution of the sources with redshift are strongly constrained and even excluded due to the non-observation of neutrinos so far.

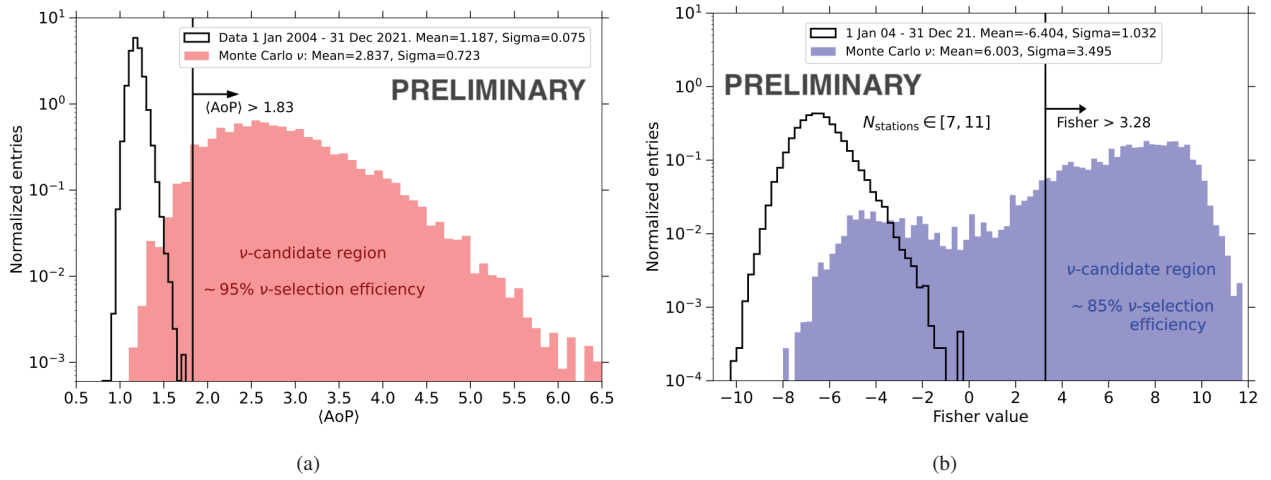


Figure 4. Results of the data unblinding shown exemplarily for two search channels; (a) ES channel, using the average area-over-peak in an SD event as discriminating observable; (b) DGH channel, in the sub-channel with $N_{\text{stations}} \in [7, 11]$, where a Fisher discriminant analysis involving several observables constructed from the individual values of area-over-peak in an SD event.

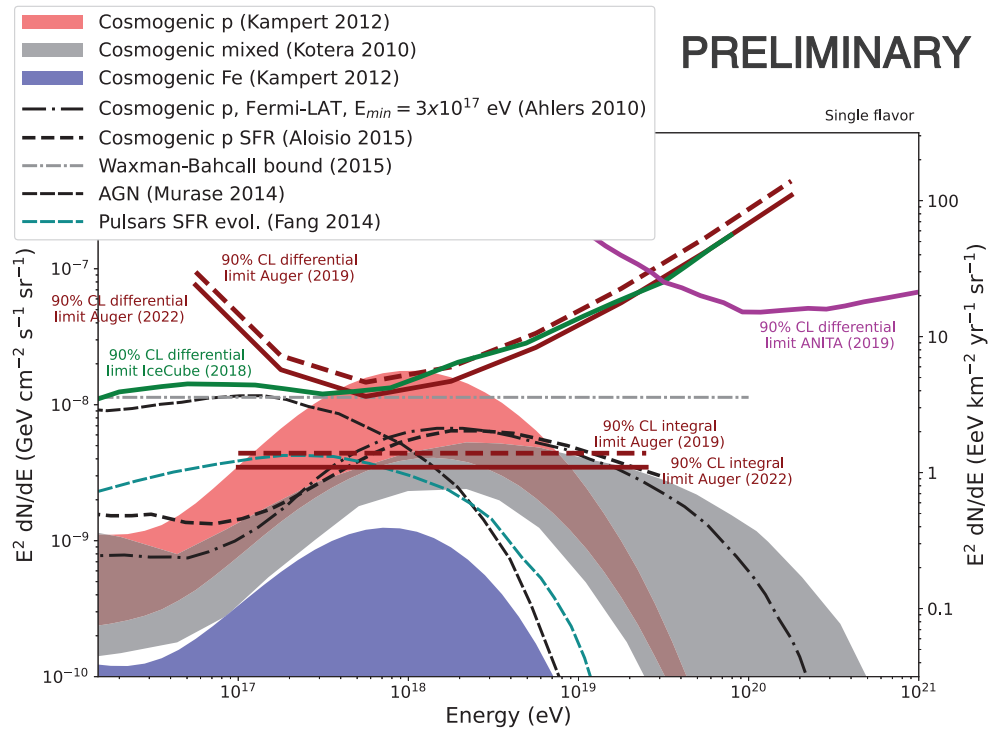


Figure 5. Updated upper limits on the diffuse flux of neutrinos, both the integral (straight solid line) as well as differential (curved solid line); for comparison, also the corresponding upper limits from [16] are shown; included are also upper limits from IceCube and ANITA and the expected neutrino fluxes under different theoretical assumptions and scenarios; for a full list of references, see [16].

However, we note that a pure-proton composition in UHE cosmic rays is already disfavored by other measurements from the Pierre Auger Observatory (see, e.g., [19]).

5 Summary and Outlook

In summary, the Pierre Auger Observatory offers an unprecedented exposure not only to UHE cosmic rays, but

also to UHE photons and neutrinos. Stringent upper limits on the diffuse flux of UHE photons and neutrinos have been obtained from the data collected by the Observatory. Here, we summarized these results and updated the upper limits on the diffuse flux of neutrinos with 3.5 more years of data, leading to an improvement of the upper limits by about 30%. Overall, these results underline that the Pierre Auger Observatory is a key actor in multimessen-

ger astronomy at the highest energies. The ongoing upgrade of the detector systems, AugerPrime [20–22], will only strengthen this role. A key part of this upgrade is the installation of scintillation detectors on top of the detector stations of the SD. The different detector responses to the electromagnetic and muonic shower components can be used to disentangle the components, from which searches for UHE photons, for example, can directly profit. In addition, the detector stations will be equipped with radio antennas to measure the radio signals emitted by an air shower, and the electronics of the SD stations will be replaced to achieve a better time resolution and a larger dynamic range. All of these efforts combined will significantly improve the upper limits or, in the best case, lead to the first unambiguous detection of a neutral particle at ultra-high energies.

References

- [1] A. Aab et al. (Pierre Auger Collaboration), Nucl. Instrum. Meth. A **798**, 172 (2015), 1502.01323
- [2] M. Risse, P. Homola, Mod. Phys. Lett. A **22**, 749 (2007), astro-ph/0702632
- [3] P. Abreu et al. (Pierre Auger Collaboration), Astrophys. J. **933**, 125 (2022), 2205.14864
- [4] P. Savina for the Pierre Auger Collaboration, PoS **ICRC2021**, 373 (2021)
- [5] P. Abreu et al. (Pierre Auger Collaboration), Article submitted to J. Cosmol. Astropart. Phys. (2022), 2209.05926
- [6] A. Aab et al. (Pierre Auger Collaboration), Astrophys. J. **789**, 160 (2014), 1406.2912
- [7] A. Aab et al. (Pierre Auger Collaboration), Astrophys. J. Lett. **837**, L25 (2017), 1612.04155
- [8] P. Ruehl for the Pierre Auger Collaboration, PoS **ICRC2021**, 973 (2021)
- [9] A. Aab et al. (Pierre Auger Collaboration), Astrophys. J. **902**, 105 (2020), 2010.10953
- [10] L. Perrone for the Pierre Auger Collaboration, these proceedings (2023)
- [11] P. Abreu et al. (Pierre Auger Collaboration), Universe **8**, 579 (2022), 2210.12959
- [12] G. Ros, A.D. Supanitsky, G.A. Medina-Tanco, L. del Peral, J.C. D’Olivo, M.D. Rodriguez-Frias, Astropart. Phys. **35**, 140 (2011), 1104.3399
- [13] P. Savina, C. Bleve, L. Perrone, Proc. 36th International Cosmic Ray Conference (Madison, USA) **PoS (ICRC2019)**, 414 (2019)
- [14] P. Abreu et al. (Pierre Auger Collaboration) (2022), 2203.08854
- [15] P. Abreu et al. (Pierre Auger Collaboration) (2022), 2208.02353
- [16] A. Aab et al. (Pierre Auger Collaboration), JCAP **10**, 022 (2019), 1906.07422
- [17] A. Aab et al. (Pierre Auger Collaboration), JCAP **11**, 004 (2019), 1906.07419
- [18] A. Albert et al. (ANTARES, IceCube, Pierre Auger, LIGO Scientific, Virgo Collaborations), Astrophys. J. Lett. **850**, L35 (2017), 1710.05839
- [19] A. Aab et al. (Pierre Auger Collaboration), Phys. Rev. D **90**, 122005 (2014), 1409.4809
- [20] A. Castellina, Pierre Auger Collaboration (Pierre Auger Collaboration), EPJ Web Conf. **210**, 06002 (2019), 1905.04472
- [21] A. Aab et al. (Pierre Auger Collaboration) (2016), 1604.03637
- [22] C. Bérat for the Pierre Auger Collaboration, these proceedings (2023)